

Advances in the Application of Surface Drifters

Rick Lumpkin

National Oceanic and Atmospheric Administration
Atlantic Oceanographic and Meteorological Laboratory
Miami, Florida 33149
email: rick.lumpkin@noaa.gov

Tamay Özgökmen

University of Miami
Rosenstiel School of Marine and Atmospheric Science
Miami, Florida 33149
email: tozgokmen@rsmas.miami.edu

Luca Centurioni

University of California San Diego
Scripps Institution of Oceanography
La Jolla, California 92093
email: lcenturioni@ucsd.edu

Annual Reviews in Marine Science

Key words

drifters, Lagrangian observations, surface currents, transport, dispersion

Abstract. Surface drifting buoys, or drifters, are used in oceanographic and climate research, oil spill tracking, weather forecasting, search and rescue operations, calibration and validation of velocities from high-frequency radar and from altimeters, iceberg tracking, and support of offshore drilling operations. In this review, we present a brief history of drifters, from the message in a bottle to the latest satellite-tracked, multisensor drifters. We discuss the different types of drifters currently used for research and operations as well as drifter designs in development. We conclude with a discussion of the various properties that can be observed with drifters, with heavy emphasis on a critical process that cannot adequately be observed by any other instrument: dispersion in the upper ocean, driven by turbulence at scales from waves through the submesoscale to the large-scale geostrophic eddies.

1. INTRODUCTION

A surface drifting buoy, hereafter referred to as a drifter, is an instrument that approximately follows water at the ocean surface, thus providing information on ocean currents. They are differentiated from floats in that floats are designed to follow ocean currents at depth, whereas drifters remain at the surface—or, as noted by the late Bruce Warren of the Woods Hole Oceanographic Institution, “drifters float and floats sink” (LaCasce 2008, pg. 2). (However, as noted below, some floats are effectively drifters while transmitting their data at the ocean surface.) More broadly, ocean instruments can be organized into three categories: Lagrangian instruments, which passively follow the water; Eulerian instruments, which remain nearly stationary with respect to a point on the earth’s surface; and self-propelled instruments, such as ships and gliders. Drifters are a subset of the Lagrangian class of instruments and are defined by

their positive buoyancy, which constrains them to follow the two-dimensional flow at the ocean surface or near surface.

Drifters have a long history of use for purposes ranging from mapping large-scale ocean currents to following oil spills to aiding search and rescue operations, and there are a correspondingly large number of drifter types. In this article, we outline the history of drifter observations; describe presently used types of drifters and their purposes; and note some of the ongoing, cutting-edge, and future uses that drifters may fulfill.

2. HISTORY

Drifters are ideal for studying ocean currents and transport, but they present two major challenges. First, how does one track the drifters, particularly over large distances and long times that preclude visual tracking? Second, how does one design the drifter so that it is not strongly affected by direct wind and wave forcing?

The earliest drifter design sidestepped the issue of tracking by merely attempting to identify the start and end of the drifters' trajectories. This was done by placing a message in a drifting bottle, imploring the discoverer to contact the deployer with the date and location where the bottle was found. The trajectory would then be inferred from these end points. The Greek philosopher Theophrastus, a pupil of Aristotle, deployed the first known such drifting bottles to test his hypothesis that the Atlantic Ocean flows into the Mediterranean Sea (Pinsky 2013). In 1846, this technique was employed by the US Coast Survey [renamed the US Coast and Geodetic Survey in 1878, and in 1970 incorporated into the newly formed National Oceanic and Atmospheric Administration (NOAA)] to gather data on ocean currents (Pinsky 2013). Probably the most massive release of bottled messages for oceanographic purposes was orchestrated by Woods Hole Oceanographic Institution oceanographer Dean Bumpus, who oversaw the release

of more than 300,000 bottles from ships and planes along the US East Coast from 1956 to 1972 (Lippsett 2014).

Leonardo da Vinci designed weighted rods attached to floating bladders in order to measure the speed of streams (IOC & WMO 1988). He tracked the drifters visually, measuring their displacements as a function of time in order to measure the structure and variability of currents in the streams and to estimate the overall transports of the streams.

In the twentieth century, a number of researchers wished to observe how the ocean surface is mixed at small scales. Richardson & Stommel (1948), attempting to validate Richardson's so-called $4/3$ rd law (Richardson 1926), deployed pieces of parsnips trimmed to 2 cm in diameter and tracked these vegetable drifters using an optical device on a pier. After attempting to release dye tracers and visually tracking the results from an airplane, Stommel (1949) found that the dye patches diffused too rapidly to track. He concluded that an array of drifters would be the ideal tool to quantify the relevant mixing processes. He first tried inflating weather balloons with seawater but found that the logistics of inflating them resulted in too small an array. He settled on releasing hundreds of pieces of standard mimeograph paper, visually tracked them from an airplane, and concluded that Richardson's $4/3$ rd law applied to ocean stirring at scales from 20 cm to tens of meters.

Visual tracking is sufficient for relatively small numbers of drifters on scales of a few tens of meters, but more advanced techniques must be employed for broader scales and larger arrays. A dramatic example was conducted as part of the Coastal Ocean Dynamics Experiment (CODE) in 1981–1982, in which 164 drifters were released off the California coast and tracked by radio-direction-finding triangulation (Davis 1985). Satellite tracking of surface drifters opened the possibility of global- scale studies. This was done first by using Nimbus satellites and

later by using the more accurate Argos Data Collection and Location System carried aboard NOAA's Television Infrared Observation Satellite N (TIROS-N) polar orbiting satellites (Lumpkin & Pazos 2007). One of the earliest deployments of satellite-tracked drifters was in 1975, as part of the North Pacific Experiment (McNally et al. 1983). A large array of more than 300 Argos-tracked drifters was deployed as part of the Global Atmospheric Research Program (GARP) First GARP Global Experiment (FGGE) in 1979–1980 in the Southern Ocean (Garrett 1980) to improve marine forecasting efforts (IOC & WMO 1988). Many drifters now rely on the extremely accurate Global Positioning System (GPS) for location, with data transmission using satellite systems such as Iridium.

A drifter consisting solely of a surface float provides velocities that are a mix of surface drift, Stokes drift, and direct wind forcing. As a consequence of the latter two, which typically have large vertical shears near the surface, the water-following characteristics of various surface float designs can vary widely. To minimize motion with respect to drift beneath the surface-wave-driven Stokes layer and remain unaffected by direct wind forcing, drifter designs typically include a sea anchor, also known as a drogue, centered at a target depth beneath the surface. For example, the FGGE drifter design consisted of a surface cylinder with a 100-m chain, with the chains on some drifters tethered to a window-shade drogue centered at a depth of 30 m. A variant of the FGGE drifter, deployed in the North Pacific to study subinertial wind forcing, had a parachute drogue centered at 30 m (McNally et al. 1989). However, a parachute drogue moving with the flow tends to collapse, whereas a window-shade drogue can twist and sail, and there are no observable differences between drifters with either of these drogue designs and drifters without drogues (see Niiler & Paduan 1995 and references therein).

As shown by Niiler et al. (1987), the most important characteristics to minimize the slip of the drifter with respect to water at the drogue depth are (a) low tension between the surface buoy and drogue, which helps eliminate Stokes drift, and (b) a large drag area for the drogue compared with all other components (Niiler et al. 1987). Niiler et al. (1987) defined a modern drifter as one with a drag area ratio (the ratio of the drogue cross-sectional area to the area of all other components) of at least 40:1, many times larger than the ratio of an FGGE- or McNally-type drifter.

Niiler & Paduan (1995) compared the motion of the effectively undrogued FGGE- type drifters with the motion of Surface Velocity Program (SVP) drifters with much larger drogues (see Section 3.1) in the North Pacific and found that 20–40% of the variance between the two sets of velocities could be accounted for by a simple linear model of wind slip superimposed on the SVP drifter velocities.

3. MODERN DRIFTER DESIGNS

3.1 The Surface Velocity Program Drifter

By the early 1980s, several different drifter designs were being used for regional studies (with FGGE being a prominent example). The oceanographic community recognized that a global array of drifters would be invaluable for oceanographic and climate research, but large variations in the water-following characteristics of the different drifter types, as well as the high costs and difficulty of deploying some designs, precluded a natural evolution from regional arrays to a global array (WCRP 1988, Niiler 2001, Lumpkin & Pazos 2007). The development of a standardized, low-cost, lightweight, easily deployed drifter with a semirigid drogue took place under the SVP, part of the Tropical Ocean Global Atmosphere experiment and the World Ocean Circulation Experiment. This effort was funded by NOAA, the US Office of Naval Research,

and the US National Science Foundation. Competing designs were submitted by NOAA's Atlantic Oceanographic and Meteorological Laboratory (AOML), the Massachusetts Institute of Technology's Draper Laboratory, and Scripps Institution of Oceanography (SIO) (Niiler 2003). The AOML design was an ~1-m-long surface cylinder float tethered to a "holey-sock" drogue—a collapsible, sectioned nylon tube supported by circular tubing. This design maximized easy shipping and deployment and had been used in tropical Pacific drifter deployments since February 1979. The SIO design had a spherical surface float and a tristar drogue—a radar-reflector-shaped drogue with three orthogonal segments—designed for optimal water-following characteristics. Ultimately, the SVP drifter design that emerged (Sybrandy & Niiler 1992) combined the holey-sock drogue of the AOML drifters centered at a depth of 15 m with reinforced tether ends and the surface float from the SIO design. This drifter (**Figure 1** became the foundation for the global drifter array of NOAA's Global Drifter Program (GDP; <http://www.aoml.noaa.gov/phod/dac>). The holey-sock SVP drifter has a drag area ratio of 40:1, with a downwind slip estimated at 0.7 cm/s per 10 m/s of wind speed for wind speeds up to 10 m/s (Niiler & Paduan 1995). Once the drogue is lost, this slip increases to nearly 9 cm/s per 10 m/s of wind (Pazan & Niiler 2001).

To reduce costs and achieve the Global Ocean Observing System goal of 1,250 drifters worldwide (see Lumpkin et al. 2016), a mini-SVP drifter design was introduced in 1992. This design retains the same water-following characteristics but has lighter, smaller components that reduce manufacturing and shipping costs (Lumpkin & Pazos 2007). Not counting drifters that are picked up or run aground, the average life (or, specifically, the half-life) of a mini-SVP drifter is ~450 days. An SVP drifter that measures sea surface temperature (SST) and drogue presence costs approximately US \$1,800.

Originally, drogue detection on SVP drifters was conducted from submergence observations collected at the surface float, as the drogue frequently pulls the surface float underwater, whereas a drogueless float remains at the surface. However, challenges to interpreting submergence records in the 2000s resulted in many drogueless drifters being inadvertently flagged as drogued; a large-scale reanalysis of the SVP data in 2012–2013 resulted in many earlier drogue losses being identified from anomalous downwind motion and from variations in transmission frequency (Lumpkin et al. 2013). SVP drifters today have replaced submergence with tether strain sensors, and the other evaluations discussed by Lumpkin et al. (2013) are also used operationally for robust drogue detection. As more drifters use GPS, additional criteria such as time to first fix are being evaluated for real-time drogue detection.

In addition to the GDP and its national and international partners that do the bulk of drifter deployments worldwide, numerous operational agencies deploy SVP- type drifters for various purposes. The US Naval Oceanographic Office deploys 20– 30 standard SVP drifters annually to support marine weather forecasts and naval operations. The International Ice Patrol (<http://www.navcen.uscg.gov/iip>), established in 1913 after the 1912 sinking of the *Titanic*, deploys 12–15 SVP drifters annually with drogue depths of 15 m and 50 m in order to track icebergs in the Labrador Sea and North Atlantic.

3.2 The Coastal Ocean Dynamics Experiment Drifter and Self-Locating Datum Marker Buoy

The CODE drifter (a.k.a. Davis drifter) was developed by SIO oceanographer Russ E. Davis (Davis et al. 1982, Davis 1985) (**Figure 2**). The design attempts to minimize Stokes drift and direct wind forcing while following the near-surface (~1- m-deep) flow. A CODE drifter consists of a central vertical tube containing a radio or satellite transmitter, an antenna, and

batteries, with four vanes attached to 50-cm-long arms that form a cruciform drogue (Davis et al. 1982, Davis 1985). At the end of each arm, a surface float is attached by 30 cm of line; the drogue extends from 30 cm beneath the surface to 120 cm (i.e., the vanes are 90 cm vertically).

The CODE drifter design has proven to be very popular in studies of ocean circulation, plankton and outflow dispersion, and oil spill modeling owing to its design focus on the upper-1-m flow. The original CODE drifters used radio triangulation, whereas modern versions typically use GPS and Iridium satellite data transmission. Post-CODE examples are plentiful in the literature; notable examples include arrays in the northern Gulf of Mexico (Sturges et al. 2001) and the Strait of Gibraltar (Sotillo et al. 2016) that focus on improving oil spill modeling, and an array off Martha's Vineyard (Rypina et al. 2014b) for calibrating and validating radar-derived velocities.

Minor variants of the CODE drifter design are routinely used for search and rescue operations; in this context, the drifters are called self-locating datum marker buoys. Every year, the US Coast Guard deploys several hundred of these buoys from ships or by air in response to search and rescue operations, and it notes that the resulting data are also valuable models of sea surface currents (US Coast Guard 2013). The US Naval Oceanographic Office deploys ~50 self-locating datum marker buoys annually.

3.3 The Lagrangian Submesoscale Experiment Drifter

A new type of drifter was recently developed for ocean sampling on a massive scale. The primary motivation for a new design emerged during the Grand Lagrangian Deployment, which was conducted in the Gulf of Mexico to explore surface flows (Olascoaga et al. 2013, Poje et al. 2014, Berta et al. 2015, Curcic et al. 2016) in the aftermath of the *Deepwater Horizon* oil spill (Crone & Tolstoy 2010). During the Grand Lagrangian Deployment, approximately 300 CODE

drifters were released in the northern Gulf of Mexico over ten days. This deployment revealed several logistical challenges regarding the volume and assembly time of the drifters that effectively limited larger-scale synoptic deployments in future expeditions. A new drifter was subsequently designed (*a*) to be compact and light, making it easy to transport and to store and handle on research vessels; (*b*) to consist of as few parts as possible, so that it could be produced by using few suppliers and assembled quickly before deployment; (*c*) to be mass producible by machines; (*d*) to be cost effective, so that very large numbers (hundreds to thousands) could be deployed in a single experiment; and (*e*) to be almost entirely biodegradable, in order to minimize long-term damage to the environment during ocean sampling.

Figure 3a shows the final design of this drifter. It consists of a floating torus that houses a GPS unit with batteries, along with a drogue. The external diameter of the torus is 0.35 m, and the drogue consists of two interlocking square pieces with a side length of 0.42 m. The torus and drogue are connected to each other by a 0.15-m natural rubber hose. The total height of the drifter below the water surface is ~0.60 m. In light of hundreds of laboratory experiments conducted in wave tanks (**Figure 3b**) using three-dimensional (3-D) printed versions of this drifter, the torus design emerged as the one that minimizes wind drag while following the water surface very accurately. The torus is also difficult to detect from a distance, reducing the chances that drifters will be picked up by fishers and boaters, which is a major problem for experiments in which a large number of drifters are deployed in close proximity for statistical descriptions of dispersion. The flexible rubber connector is a critical design element to virtually eliminate wave rectification caused by Stokes drift.

Because the laboratory can differ significantly from the ocean in terms of wave characteristics, winds, currents, and buoyancy fluxes near the surface, drift characteristics have

also been tested in the ocean. Novelli et al. (2016) found that the motion of this drifter is virtually the same as that of the CODE drifter.

The main material used to construct the drifter is Metabolix corn-based bioplastic with an expected structural stability of approximately four to six months in the ocean. The drifter is mass produced by injection molding, and the two parts of the torus are spin welded together in order to avoid the use of toxic glue. It weighs 4 kg and is 95% biodegradable in the ocean; the only components that are not biodegradable are the GPS board and the batteries. Globalstar SPOT Trace satellite trackers are presently being used to obtain positions every 6 min, with an error of 6 m. These figures are critical for dispersion estimates over the submesoscale range (Haza et al. 2014). The battery life of the drifter at this transmission rate is approximately three months, which is capped by the period of biodegradation. Thus, this drifter is intended mainly for detecting and mapping submesoscale processes in the ocean for basic research, as well as for use in responses to hazardous material spills in the ocean. Approximately 1,000 of these drifters were deployed in the Gulf of Mexico in the winter of 2016 (**Figure 4**) for the Lagrangian Submesoscale Experiment (LASER); this included a launch of 300 drifters over a submesoscale eddy over 8 h, demonstrating that massive-scale rapid ocean sampling is feasible using these drifters.

3.4 Undrogued Drifters and Surfaced Floats

Undrogued drifter motion is a mix of surface drift, Stokes drift, and windage. This motion can also be expected of a profiling Argo float while at the surface and transmitting data. In the near-inertial band, where the surface drift dominates, Argo float surface trajectories can be used to map inertial oscillation amplitudes (Park et al. 2004, 2005). The surface velocities of Argo floats are included in the YoMaHa'07 data set (Lebedev et al. 2007). This ancillary Argo

data is becoming less valuable as the Argo array transitions from Argos to Iridium data transmission, as the latter requires far less time at the surface.

Several drifter manufacturers continue to offer drogueless drifters for various purposes. As noted above, the water-following characteristics of such designs can vary widely as a function of relatively minor changes in buoyancy, float shape, and so on.

Offshore oil and gas drilling operations can be adversely affected by strong currents (more than half a knot), with extremely large economic impacts. Arrays of drifters are used operationally to calibrate and initialize ocean models in order to support these operations. The largest operation of this nature is the EddyWatch service (<http://www.horizonmarine.com/eddywatch.html>), for which an extensive array of self-built drifters are deployed annually (B. Woodward, personal communication).

4. MEASURING OCEAN CURRENTS WITH DRIFTERS

4.1 Mapping Large-Scale Ocean Currents

As summarized by Lumpkin & Johnson (2013) and Maximenko et al. (2014), a large number of regional, basin-scale, and global studies have used drifter data to map ocean circulation patterns and their variations at monthly to interannual timescales. This is typically done by pseudo-Eulerian mapping, in which the drifter observations are grouped and averaged in spatial bins. In the simplest approach, the bins are a regular grid, and the mean velocities in each bin are a simple average of the observations. More sophisticated approaches address the spatial and/or temporal variations of the observations within the bin (Bauer et al. 1998, Johnson 2001, Lumpkin & Johnson 2013) or the decorrelation timescale of the observations (Lumpkin 2003), or

cluster the observations rather than using fixed-sized bins to reflect the inhomogeneous spatial distribution of data density (Koszalka et al. 2011).

4.2 Studying Mesoscale Variability

Many drifter deployments have targeted eddy features so that their structure and evolution can be observed from the subsequent trajectories, and many researchers have identified opportunistic sampling in the historical data base to make similar calculations. Studies frequently derive a large-scale flow as described in Section 4.1, then interpolate and remove those velocities from the instantaneous velocities of the individual drifters to derive eddy velocities, which can then be used to calculate properties such as eddy kinetic energy and terms in the energy budget (e.g., Lumpkin & Flament 2013). If the study is concerned with geostrophic variability, care must be taken to remove near-inertial oscillations, which could otherwise dominate much of the eddy kinetic energy in the Lagrangian velocity time series. The literature of peer-reviewed studies using drifters to examine mesoscale variability is vast; AOML (2016) maintains a comprehensive list of such studies.

4.3 Subinertial Wind-Driven Variability

Drifter studies of wind-driven variability often remove the geostrophic velocity, estimated from hydrography or satellite altimetry; low-pass filter the resulting drifter velocity anomalies to remove inertial and higher-frequency motion; and regress the results onto wind speed or wind stress. Notable examples of this include studies by Ralph & Niiler (1999) and Rio & Hernandez (2003). Ralph & Niiler (1999) carried out the first study to derive a robust Ekman spiral in observations spanning the tropical and subtropical Pacific basin, by binning the results as a function of the SVP drogue depth (15 m) divided by the local depth of the Ekman layer. Rio

& Hernandez (2003) extended this result to determine the spatial and seasonal variability of the Ekman model parameters, the Ekman depth, and the vertical eddy viscosity. Elipot & Gille (2009) examined the frequency response of drifter motion to wind forcing (i.e., the transfer function of wind energy into the upper ocean) separately for cyclonic and anticyclonic motion.

4.4 Inertial and Superinertial Motion

Few drifter studies in the pre-GPS period focused on motion at inertial or higher frequencies over many periods. Until the early 2000s, Argos location fixes (dependent on the constellation of satellites with the Argos system) were limited to a few per day at maximum. As a consequence, and to save power, most of the drifters in the global SVP array had a duty cycle of one day on, two days off (Lumpkin & Pazos 2007). As the Argos constellation grew, the frequency of fixes increased, and GDP drifters increasingly switched to an always-on duty cycle. By early 2005, with the advent of multisatellite processing, the frequency of global observations increased to nearly hourly (Elipot & Lumpkin 2008). Elipot et al. (2016) took advantage of this to derive a global product of regular hourly drifter locations and velocities and their formal errors since January 2005, for studies of inertial, tidal, submesoscale, and superinertial motion.

With the introduction of GPS tracking, numerous studies have taken advantage of rapid position sampling to observe motion at much smaller scales than was previously possible. For example, arrays of small GPS-tracked drifters, designed to float similarly to a human, have been deployed in the near surf zone to study rip currents (see Schmidt et al. 2003, Brown 2008). These observations have been used to map the structure of rip current cells, which evolve with a characteristic timescale comparable to the orbital period of the drifters in the cells (Brown 2008). The GDP global drifter array is currently transitioning from Argos to Iridium, with on-the-hour GPS positions for all drifters.

4.5 Calibrating and Validating High-Frequency Radar Measurements

Drifters are routinely used for calibration, validation, and error estimation of velocities derived from coastal high-frequency radar sites (e.g., Paduan & Rosenfeld 1996, Kaplan et al. 2005). Recent examples include a study by Lipa et al. (2009), who used an array of 42 drifters with tristar drogues at 1-m depth to evaluate radar-derived velocities outside the mouth of San Francisco Bay. They found a mean standard deviation between these velocities of 8.5 cm/s, comparable to the estimated error in radar velocities. Ohlmann et al. (2007) repeatedly deployed an array of similar drifters to evaluate radar-derived velocities off Santa Barbara and San Diego and found that velocity differences were far from stationary, in one case growing from ~ 0 cm/s to >20 cm/s in 1 h. Rypina et al. (2014b) compared velocities from an array of 80 CODE-style drifters with high-frequency radar velocities off Martha's Vineyard and found that the averaged radar-derived velocities were unbiased in direction but too weak by ~ 2 cm/s. They also compared simulated drifters, advected by the radar-derived velocity field, to the actual trajectories and found that the two diverged by 1 km over ~ 10 h.

4.6 Calibrating Satellite-Derived Ocean Currents

Drifters are valuable for in situ calibration and validation of satellite-derived surface currents. Lagerloef et al. (1999) created a surface current model derived from satellite altimetry and winds (for the geostrophic and Ekman flows, respectively), with coefficients tuned to match currents derived from SVP drifters. They noted that the Ekman-removed drifter velocities were on average 1.4 times faster than the altimeter-derived geostrophic currents, which they attributed to smoothing of the altimetric sea height anomalies or to wind-driven motion correlated with geostrophic velocity anomalies. Niiler et al. (2003) removed the Ekman component from low-passed drifter velocities in the northwestern Pacific using the Ralph & Niiler (1999) model and

compared the resulting velocity anomalies with geostrophic velocity anomalies derived from Archiving, Validation, and Interpretation of Satellite Oceanographic Data (AVISO) altimetry. They showed that an unbiased time-mean current field could be derived from a synthesis of drifters and altimetry, taking advantage of the homogeneous-in-time AVISO fields and the absolute velocity measured by the drifters. They also derived a set of coefficients that, when multiplied by the AVISO geostrophic velocity anomalies, best matched the Ekman- removed drifter-derived eddy kinetic energy. Following this approach, Lumpkin & Garzoli (2011) showed that the Brazil-Malvinas Confluence of the southwestern Atlantic shifted significantly southward during the early 2000s and suggested that this was due to increased advection of anomalously water from the Indian Ocean. Also following this approach, Hormann et al. (2012) examined interannual variations of the Atlantic North Equatorial Countercurrent and related these variations to the zonal and meridional climate modes of the basin.

4.7 Studying Floating Marine Debris

Several recent studies have used SVP drifter observations to better understand the ocean advection pathways of floating marine debris, such as plastics. Maximenko et al. (2012) used statistics derived from drifter trajectories to run forward in time an initially homogeneous distribution of particles at the ocean surface and showed that the particles accumulate in five zones matching regions of observed enhanced marine debris. Lumpkin et al. (2012) extended the Maximenko et al. (2012) study to include the observed odds of drifters running aground, in order to determine locations most prone to marine debris washing ashore. Van Sebille et al. (2015) ran similar projections with more realistic initial conditions for plastic release, calibrated the arbitrary units of the simulation to observed plastic densities, and found that the total amount of

floating plastic debris is only ~1% of the current best estimate of the plastic waste entering the ocean.

5. MEASURING OCEAN TEMPERATURES WITH DRIFTERS

In situ SST measurements are critical for reducing biases in satellite-derived temperatures (e.g., Emery et al. 2001, Zhang et al. 2009) and thus for determining interannual variations and long-term trends in the earth's surface temperature. Fixed-point surface temperature measurements are limited to land stations, near-coastal moorings, and the tropical band covered by the Global Tropical Moored Buoy Array. SST measurements from ships are limited primarily to the major shipping lanes, leaving vast segments of the world's oceans—particularly the southern sectors of the Atlantic, Pacific, and Indian Oceans and the entirety of the Southern Ocean—unsampled except by drifters. The ~450-day lifetime of the SVP drifters is sufficient for them to cover these otherwise unsampled regions. As a consequence, temporal variations in the maximum potential bias in satellite-derived SST from all observations in the Global Ocean Observing System (ships, moored buoys, and drifters) since 2000 are strongly negatively correlated with the number of drifters in the GDP global drifter array (Zhang et al. 2009). All of the drifters in the global array measure SST at 10–20 cm beneath the surface using a thermistor near the base of the surface float. These data are transmitted via the Global Telecommunication System for climate monitoring and assimilation in numerical weather prediction and ocean forecasting models.

Kennedy et al. (2012) used collocated in situ and satellite observations to determine that there is a random error of 0.26 K in drifter SST measurements, compared with 0.7–1.2 K for ships (Kent & Challenor 2006, Kennedy et al. 2012). Several studies have shown that drifter measurements are approximately unbiased, whereas ship temperatures (particularly those from

engine intakes) are biased warm (e.g., Emery et al. 2001, Kennedy et al. 2012). To improve the accuracy of drifter SST measurements, several GDP drifters have been upgraded with thermistors to measure SST with an accuracy of 0.05 K, at a resolution of 0.01 K (see GHRSSST 2011). These data are currently being evaluated.

6. OTHER PROPERTIES THAT CAN BE MEASURED BY DRIFTERS

The GDP array offers a unique opportunity to measure oceanic and atmospheric variables on a global scale because new sensors can be added to the basic SVP design. Therefore, through the years, several variants of the SVP drifter have been developed.

6.1 The Surface Velocity Program Barometer Drifter

The SVP barometer (SVPB) drifter has the same characteristics as the SVP drifter (i.e., a drogue centered at 15-m depth and a thermistor to measure SST) but also carries a barometer, usually a high-precision barometer by Honeywell with an rms accuracy of 0.4 hPa (Niiler 2001, Centurioni et al. 2016). Because the drifter's hull is often pulled underwater when surface waves are present, the air intake that connects the air pressure sensor with the atmosphere is protected by a self-draining port and by Gore-Tex or equivalent air-permeable screens. The air pressure is sampled at 1 Hz, and the data are cleaned by the onboard digital controller (to remove the erroneous reading when the drifter hull is underwater), averaged, and formatted for satellite transmission. Most SVPB drifters have an Iridium satellite transmitter because the Iridium system has a much lower data latency than the Argos system, which greatly benefits numerical weather prediction applications because the assimilation window for real-time sea level pressure data ranges between 3 and 6 h. The lower the data latency is, the more data are available to constrain weather forecasting models. As the data are received nearly in real time, they are

distributed globally on the Global Telecommunication System. Approximately 50% of the GDP array is composed of SVPB drifters; Centurioni et al. (2016) discussed the ways in which drifter data have significantly improved weather forecasting numerical models.

6.2 The Minimet Drifter

Another variant of the SVPB drifter, called the Minimet, is designed to measure wind velocity at sea level, especially within tropical cyclones. The early version of the Minimet used hydrophones to infer wind speed from ambient noise and used a swivel-attached surface float with a wind vane and a compass to compute wind direction. However, this methodology was phased out because the ambient noise reading quickly saturated for hurricane-force winds. The modern version of the Minimet uses a sonic anemometer that measures the wind velocity in the range of 0– 60 m/s, with a 2° resolution for the wind direction (Hormann et al. 2014a). Minimet drifters are often air deployed in front of tropical cyclones.

6.3 The Autonomous Drifting Ocean Station

Autonomous drifting ocean stations (ADOSs) are also used in air-ocean interaction studies in tropical cyclone conditions. Ocean stratification is believed to play an important role in setting the enthalpy fluxes that determine the intensification or dampening of tropical storms (D'Asaro et al. 2013). The surface expression of the ADOS is similar to that of the Minimet drifter, the only difference being that the hull of the ADOS has a larger buoyancy reserve. Beneath the surface float is a 200-m- long thermistor chain with temperature and pressure sensors typically spaced at 10-m intervals to measure ocean stratification and the heat potentially available for changing the intensity of the storm. A combination of ADOSs and Minimet drifters are usually deployed in linear arrays approximately 300–400 km long in front of the path of

tropical cyclones (D'Asaro et al. 2013, Hormann et al. 2014a). The ADOS is not a Lagrangian instrument, because it has no drogue, and the water velocity relative to the submerged thermistor chain can be significant (Centurioni 2010). Similar drifters, also carrying vertical profiling acoustic current meters, have been used successfully to study large-amplitude nonlinear internal waves (Centurioni 2010).

6.4 The Surface Velocity Program Salinity Drifter

The SVP salinity (SVPS) drifter designed at SIO is a Lagrangian drifter drogued at 15-m depth that carries a Sea-Bird SBE 37-SI conductivity sensor integrated into the hull. Recent studies have shown that SVPS drifters can provide stable salinity data at 0.45-m depth for as long as one year (Hormann et al. 2014b). The SVPS drifters are significantly more expensive than the simpler SVP and SVPB drifters and are normally deployed in smaller numbers for process studies, for example, in conjunction with satellite salinity missions such as Aquarius (Centurioni et al. 2015).

6.5 The Surface Velocity Program Wave Drifter

Recent technical developments have shown that commercial GPS engines sampled at a sufficiently high rate (typically between 2 and 5 Hz) can provide a reasonably accurate description of the directional spectra of surface gravity waves (e.g., Herbers et al. 2012). Commercial versions of wave riders that use GPS technology also exist.

The SVP wave (SVPW) drifter uses firmware developed at SIO to compute onboard the directional wave spectra parameters once every hour. Several SVPW units have already been deployed in the open ocean. The SVPW drifter performs best when the drogue is not present. At the moment, SVPW drifters can receive a command through the Iridium satellite network that

activates the wave sampling part of the firmware once a drifter loses its drogue. Because a large portion of the GDP array is made of undrogued drifters, there is an opportunity to quickly implement a global array of SVPW drifters in an opportunistic fashion.

7. MEASURING OCEAN DISPERSION WITH DRIFTERS

Lagrangian dispersion is readily understood by anyone who has thrown a leaf in a pond. A wide range of applied problems require addressing several questions, including where substances come from, where they go, and how fast they spread. These questions involve the dispersion of biogeochemical tracers in the ocean as well as pollutants from marine oil spills, such as those from the Ixtoc I spill in 1979 (Jernelöv & Lindén 1981) and the *Deepwater Horizon* spill in 2010 (Crone & Tolstoy 2010). Such spills have a socioeconomic impact on the order of tens of billions of dollars (Heavey et al. 2015). Rapid release of radioactive materials into the ocean by catastrophic accidents, as in the case of the Fukushima meltdown (Rypina et al. 2014a), and slow seeps in coastal regions (Staletovich 2016) also constitute dispersion problems. The increasing density of intercontinental airline traffic and the use of larger planes result in marine accidents (Normile 2014), for which predicting where debris came from can potentially save lives. The US Coast Guard regularly deploys drifters in the ocean for search and rescue missions. A lack of understanding of dispersion processes and stresses on water resources can threaten the water supplies of entire cities (McCarty 2015).

7.1 Scientific Approaches to Dispersion

There are several scientific ways to think about the Lagrangian dispersion problem. As in classical physics, these can be generally classified as either statistical or deterministic methods. Taylor (1921) was the first to quantify the motion of Lagrangian particles as a diffusivity

coefficient. Shortly thereafter, Richardson (1926) noted that turbulent flows consist of eddies of different scales l with different characteristic speeds U . As such, the diffusivity $K \sim Ul$ must be a function of spatial scale, as opposed to being constant, as implied by Taylor (1921). Empirically, Richardson (1926) arrived at his 4/3rd law, $K \sim l^{4/3}$, which was shown to have a striking validity for lakes and coastal oceans (Okubo 1970). From dimensional analysis, $D^2 \sim \varepsilon l^3$, where D is a two-particle or relative dispersion (Boffetta & Sokolov 2002) and ε is the kinetic energy dissipation rate. Thus, Richardson's dispersion law implies that ε is constant, in remarkable agreement with the fundamental underpinnings of the 3-D turbulence theory by Kolmogorov (1941). These findings have stimulated research for many decades on the nature of the dispersion of a tracer encountering eddies of different sizes in turbulent flows; Monin & Yaglom [1965 (2007)], Bennett (1984), Babiano et al. (1990), and La Casce (2008) have published extensive reviews on this subject. It is important to note that implicit in these statistical descriptions is the assumption of homogeneity, isotropy, and stationarity that may not always hold true in the ocean. Also, statistical laws cannot be used to make predictions for specific events.

A completely different, deterministic approach was developed for Lagrangian dispersion on the basis of dynamical system theory (Ottino 1989). The fundamental concept in these approaches is that Lagrangian motion can be chaotic even in the presence of simple flows, just by virtue of time dependence (Aref 1984). Therefore, the basic dynamical distinction between trapping and repelling (or elliptic and hyperbolic) regions in two-dimensional (2-D) flows (Provenzale 1999) needs to be advanced by incorporating the effect of time variability. These methods, called Lagrangian coherent structures (Mezić & Wiggins 1994, Haller & Poje 1998, Haller & Yuan 2000), have found a significant use for oceanic applications (d'Ovidio et al. 2004, Olascoaga et al. 2006, Haza et al. 2007, Mancho et al. 2008), mainly because large-scale deep-

ocean flows tend to have long-lasting mesoscale coherent structures because of the effects of rotation, stratification, and a shallow aspect ratio. This results in a reduction in spatial complexity when compared with 3-D turbulence.

Although dynamical system approaches have proven to be extremely useful, they have their limitations as well. In particular, being a diagnostic technique, computation of Lagrangian coherent structures requires a full knowledge of oceanic surface flows. However, as pointed out by Sanford et al. (2011), observing oceanic flows in their full complexity is a daunting challenge. Also, as the spatial and temporal complexity of analyzed flows increases, so too does the complexity of Lagrangian coherent structures (Haza et al. 2012), making it quite difficult to distinguish which structure is more important for surface dispersion. Special methods can be devised for that purpose (Olascoaga & Haller 2012). Poje & Haller (1999) also showed that, in the presence of the slow time variability characteristic of mesoscale flows, the approximate location of hyperbolic trajectories can be estimated from stagnation points in Eulerian velocity snapshots. Finally, the transport barriers derived using these methods in 2-D flows (Haza et al. 2016) and surfaces from 3-D flows (Pratt et al. 2013, Rypina et al. 2015) are quite sensitive to fine details in the velocity fields. These findings put the robustness of these structures in question.

7.2 The Nature of Surface Flows in the Ocean

Surface flows in the ocean tend to be quite different from 3-D turbulence in classical fluid dynamics, and the deep-ocean flows in quasi-geostrophic balance. The oceanic surface velocity field is strongly influenced by the air-sea forcing. **Figure 5a** shows a striking example of how the complex interactions between the atmosphere and the ocean can shape the Lagrangian

distribution along the boundary of these large systems in the context of an oil spill. **Figure 5b** shows a general classification of transport processes near the oceanic boundary layer (OBL). At scales of 1 m to 100 m and of 1 s to a few hours, fully 3-D turbulent processes dominate the OBL dynamics. Langmuir turbulence (Leibovich & Tandon 1993, Skillingstad & Denbo 1995, D'Asaro 2001, Kukulka et al. 2010, Belcher et al. 2012, D'Asaro et al. 2014), arising from a combination of winds and waves, creates surface convergences along wind streaks. If waves are not aligned with winds, the classic structure of the Langmuir circulation can be modified significantly (Van Roekel et al. 2012). Stokes drift from surface waves and Ekman transport from the wind stress combine to form the near-surface current. The depth of this current is controlled by boundary layer turbulence, including Langmuir circulations. Convective plumes that are strongly modulated by the diurnal cycle and wind forcing also influence material dispersion at the surface. The spatial scale of these plumes scales initially with the depth of the mixed layer, but it is controlled later by rotational effects and winds (Mensa et al. 2013).

It can be quite hard to distinguish between Langmuir and convective turbulence because they are generated under similar forcing conditions (Sundermeyer et al. 2014). Nevertheless, they both seem to have a similar effect on surface dispersion in that surface material tends to collect along convergence zones created by these processes. At scales of 100 m to 10 km and $O(1)$ day, so-called submesoscale processes critically affect transport and mixing in the upper ocean (Boccaletti et al. 2007, Capet et al. 2008, Fox-Kemper et al. 2008, Thomas et al. 2008, Klein & Lapeyre 2009, Taylor & Ferrari 2010, Zhong et al. 2012). Submesoscale processes are also confined mostly to the OBL (Shcherbina et al. 2013) and demonstrate significant seasonality (Mensa et al. 2013, Sasaki et al. 2014). Frontal submesoscale eddies can move surface material across the fronts. Considering that the OBL is stirred below by the mesoscale flows, the

tremendous complexity of the processes influencing the dispersion of material near the ocean's surface becomes apparent.

The multiscale nature of the combination of these processes can make the actual distribution of material very different from the distribution that results solely from mesoscale flows at depth (Huntley et al. 2015, Jacobs et al. 2015).

7.3 Measuring Dispersion

Traditional profiling instruments [acoustic Doppler current profilers, CTD (conductivity, temperature, depth) instruments, and current meters] collect only fixed-point measurements that are not well suited to estimating dispersion by oceanic processes with high spatial complexity. Towed instruments create a compromise between vertical and horizontal coverage and are limited to the ship's location and the period of the expedition. Autonomous instruments, such as gliders, can offer a cost-effective alternative for long-term monitoring, but they are prohibitively expensive to deploy in large enough numbers to obtain good spatial coverage, and they encounter aliasing challenges owing to the lack of synoptic sampling. Dye release (Ledwell et al. 1998, 2000) is an effective tool, but observation of a dye patch from a ship becomes gradually more challenging as its size grows. A lack of synoptic sampling and the limitation of the observing period to the ship's presence are also obvious challenges here. Lidar (Sundermeyer et al. 2007) is a promising technique to detect dye but is limited to clear conditions at the sea surface and does not provide depth information; dye moves in 3-D, and there can be significant shear dispersion near the surface of the ocean.

Coastal high-frequency radar (Steward & Joy 1974; Paduan & Rosenfeld 1996; Shay et al. 2003, 2007; Kaplan et al. 2005) is a valuable tool, providing estimates of the surface velocity field down to 250 m at a 15-min resolution. However, these radars are limited to coastal regions,

their coverage at high resolution does not exceed a radius of 20 km, and simulated Lagrangian observations in high-frequency- radar-derived currents have revealed significant differences at scales smaller than 2 km and 3 h (Rypina et al. 2014b). Satellite altimeters typically have a large spacing between group tracks (Ducet et al. 2000) and suffer from along-track signal contamination by high-frequency motions (Chavanne & Klein 2010). In addition, altimeters measure sea surface height anomaly. Thus, one typically relies on the geostrophic approximation to deduce surface currents (Wunsch & Stammer 1998), whereas submesoscales and faster, smaller scales of motions are distinctly ageostrophic (McWilliams 2008). None of the above instruments measure the Stokes drift by waves, which can be significant for oceanic dispersion and transport (Curcic et al. 2016).

To our knowledge, drifters are the only instruments suited for measuring surface or near-surface dispersion, which is a Lagrangian quantity by its very nature. Drifters can be readily designed in different sizes and shapes to focus on different dispersive processes. They can be produced and deployed in large enough numbers to provide a true synoptic velocity field near the surface of the ocean. They can also stay in the ocean for long periods and survive under all oceanic conditions, including hurricanes (Curcic et al. 2016).

7.4 Findings about Ocean Dispersion

Noting the value of drifter observations, investigators have conducted several studies to identify scaling laws for dispersion in the OBL. Ocean models seem to provide an advantage in that Lagrangian particles can be placed in virtually unlimited numbers with perfect positional accuracy. However, studies using both general circulation models and fine-scale large-eddy simulations (Haza et al. 2008; Poje et al. 2010; Özgökmen et al. 2011, 2012; Özgökmen &

Fischer 2012; Mensa et al. 2013) revealed that only two main processes (general circulation and mesoscales, mesoscales and submesoscales, etc.) can be included in models at the present time owing to computational constraints, and a vast range of oceanic fluid dynamics is represented by simplifications and parameterizations. As such, the only way to find out what is really happening in nature is to conduct oceanic experiments using an increasing number of drifters with high positional accuracy. The Richardson regime has been observed at mesoscales by LaCasce & Bower (2000) (using floats for deep measurements), in the North Atlantic by Ollitrault et al. (2005), in the Gulf of Mexico by LaCasce & Ohlmann (2003) (using 15–30-m-drogued drifters), in the Nordic Seas by Koszalka et al. (2009), and in the Ligurian Sea by Schroeder et al. (2011). Studies have also found that the Richardson scaling extends into the submesoscale regime, most notably studies by Lumpkin & Elipot (2010) in the North Atlantic, Schroeder et al. (2012) in the Ligurian Sea, and Berti et al. (2011) in the Brazil Current. Using 300 drifters with a highly accurate positioning system and a high-frequency data stream, Poje et al. (2014) obtained results consistent with Richardson's $4/3$ rd law in the northern Gulf of Mexico. The authors also used a multiscale sampling module placed from three vessels simultaneously in the ocean and showed that the validity of the scaling behavior documented by Okubo (1970) extends to larger scales in the ocean. However, a more detailed analysis of the Grand Lagrangian Deployment data set by Beron-Vera & LaCasce (2016) questioned these findings, suggesting that stirring in the submesoscale range may be driven by the mesoscale (resulting in exponential rather than Richardson's law dispersion) and hypothesizing that the results of Poje et al. (2014) may be due to the presence of inertial oscillations that are quite pronounced in shallow summer mixed layers of the subtropical regions.

Therefore, the jury is still out regarding the scaling laws and the role of different dynamical processes in ocean dispersion, and bridging the gap from classical fluid dynamics to mesoscale oceanic flows will require significantly more effort. We expect that new drifter technologies will play a key role in understanding dispersion in the ocean.

7.5 Outlook

The seasonality of ocean dispersion requires deeper investigation. The depth of the OBL increases in winter because of wind forcing and cooling, which should increase the contribution of submesoscale fronts and eddies in surface dispersion, but winter is also when wind-driven transport is strongest. Winds tend to be relatively easier to predict and measure than upper-ocean processes. It remains unclear how much of the upper-ocean dispersion can be explained by winds and how much by ocean flows.

Stokes drift has been known for some time, but its role in ocean dispersion has not been quantified adequately. Stokes drift is typically not included in ocean circulation models, as this requires coupling with a computationally expensive wave model.

In addition to seasonality, the geographic dependence of ocean dispersion is a frontier that can benefit from massive-scale usage of drifters. Polar regions tend to have a small radius of deformation, compressing mesoscales and submesoscales close together. Under the strong stratification prevailing in the Arctic, one can expect internal gravity wave signals to affect dispersion in the OBL. With recent changes in the global climate, extensive waterways that were once covered by ice have opened in the Arctic. This new ocean may be explored further for oil drilling, creating the possibility of accidents in a pristine environment. Compact, biodegradable surface drifters could be the ideal instruments to quantify circulation and dispersion in that area.

8. SUMMARY

As location and data transmission technologies have improved over the last several decades, the value of drifters for research and operations has grown tremendously. Our ability to understand their water-following characteristics, at least in weak to moderate wind and wave states, has also grown tremendously owing to the work of pioneers such as the late P.P. Niiler of SIO. Since 2005, the global array of SVP drifters has spanned the world, offering inexpensive platforms for additional observations and greatly improving our ability to understand present and future climate changes. Meanwhile, the development of inexpensive, short-lived, biodegradable drifters has allowed massive deployments for robust oil spill tracking with minimal environmental impact. Although much remains to be understood— from ocean-atmosphere interactions needed to improve hurricane intensity forecasts to the qualitative nature of oceanic stirring at submesoscales—there is little doubt that drifters will play a major role in future research.

DISCLOSURE STATEMENT

The authors are not aware of any affiliations, memberships, funding, or financial holdings that might be perceived as affecting the objectivity of this review.

ACKNOWLEDGMENTS

The authors would like to thank B. Woodward for invaluable conversations that contributed to the material presented here. R.L. was supported by NOAA's Atlantic Oceanographic and Meteorological Laboratory and NOAA's Climate Program Office. T.Ö. is grateful for the generous support of the Gulf of Mexico Research Initiative through the Consortium for Advanced Research on Transport of Hydrocarbon in the Environment. L.C. was

funded by NOAA grant NA10OAR4320156 (“The Global Drifter Program”). We thank Cedric Guigand, Edward Ryan, and Eric D’Asaro for their help in preparing **Figures 3, 4, and 5**, respectively.

LITERATURE CITED

AOML (Atl. Oceanogr. Meteorol. Lab.). 2016. *Drifter bibliography research papers*. Updated Apr. http://www.aoml.noaa.gov/phod/dac/gdp_biblio.php

Aref H. 1984. Stirring by chaotic advection. *J. Fluid Mech.* 192:115–73

AVISO (Arch. Valid. Interpret. Satell. Oceanogr. Data). 2016. *One thousand drifters and one future satellite in the Gulf of Mexico*. Image of the Month, Apr.

<http://www.aviso.altimetry.fr/en/news/idm/2016/apr-2016-one-thousand-drifters-and-one-future-satellite-in-the-gulf-of-mexico.html>

Babiano A, Basdevant C, Leroy P, Sadourny R. 1990. Relative dispersion in 2- dimensional turbulence. *J. Fluid Mech.* 214:535–57

Bauer S, Swenson MS, Griffa A, Mariano AJ, Owens K. 1998. Eddy–mean flow decomposition and eddy-diffusivity estimates in the tropical Pacific Ocean. 1. Methodology. *J. Geophys. Res.* 103:30855–71

Belcher SE, Grant ALM, Hanley KE, Fox-Kemper B, Van Roekel L, et al. 2012. A global perspective on Langmuir turbulence in the ocean surface boundary layer. *Geophys. Res. Lett.* 39:L18605

Bennett AF. 1984. Relative dispersion—local and nonlocal dynamics. *J. Atmos. Sci.* 41:1881–86

Beron-Vera F, LaCasce JH. 2016. Statistics of simulated and observed pair separation in the Gulf of Mexico. *J. Phys. Oceanogr.* In review.

- Berta M, Griffa A, Magaldi M, Özgökmen TM, Poje AC, et al. 2015. Improved surface velocity and trajectory estimates in the Gulf of Mexico from blended satellite altimetry and drifter data. *J. Atmos. Ocean. Technol.* 32:1880–901
- Berti S, Santos FAD, Lacorata G, Vulpiani A. 2011. Lagrangian drifter dispersion in the Southwestern Atlantic Ocean. *J. Phys. Oceanogr.* 41:1659–72 Boccaletti G, Ferrari R, Fox-Kemper B. 2007. Mixed layer instabilities and restratification. *J. Phys. Oceanogr.* 37:2228–50
- Boffetta G, Sokolov I. 2002. Relative dispersion in fully developed turbulence: the Richardson's Law and intermittency corrections. *Phys. Rev. Lett.* 88:094501
- Brown J. 2008. *Lagrangian field observations of rip currents*. Master's Thesis, Univ. Delaware, Newark
- Capet X, McWilliams J, Molemaker M, Shchepetkin A. 2008. Mesoscale to submesoscale transition in the California Current System: I. Flow structure, eddy flux and observational tests. *J. Phys. Oceanogr.* 38:29–43
- Centurioni LR. 2010. Observations of large-amplitude nonlinear internal waves from a drifting array: instruments and methods. *J. Atmos. Ocean. Technol.* 27:1711–31
- Centurioni LR, Horanyi A, Cardinali C, Charpentier E, Lumpkin R. 2016. A global observing system for measuring sea level atmospheric pressure: effects and impacts on numerical weather prediction. *Bull. Am. Meteorol. Soc.* In revision.
- Centurioni LR, Hörmann V, Chao Y, Reverdin G, Font J, Lee D-K. 2015. Sea surface salinity observations with Lagrangian drifters in the tropical North Atlantic during SPURS: circulation, fluxes, and comparisons with remotely sensed salinity from aquarius. *Oceanography* 28(1):96–105

- Chavanne C, Klein P. 2010. Can oceanic submesoscale processes be observed with satellite altimetry? *Geophys. Res. Lett.* 37:L22602
- Crone T, Tolstoy M. 2010. Magnitude of the 2010 Gulf of Mexico oil leak. *Science* 330:634
- Curcic M, Chen S, Özgökmen TM. 2016. Hurricane induced ocean waves and Stokes drift and their impacts on surface transport and dispersion in the Gulf of Mexico. *Geophys. Res. Lett.* 43:2773–81
- D’Asaro EA. 2001. Turbulent vertical kinetic energy in the ocean mixed layer. *J. Phys. Oceanogr.* 31:3530–37
- D’Asaro EA, Black PG, Centurioni LR, Chang YT, Chen SS, et al. 2013. Impact of typhoons on the ocean in the Pacific. *Bull. Am. Meteorol. Soc.* 95:1405-18 D’Asaro EA, Thomson J, Shcherbina AY, Harcourt RR, Cronin MF, et al. 2014. Quantifying upper ocean turbulence driven by surface waves. *Geophys. Res. Lett.* 41:102–7
- Davis RE. 1985. Drifter observations of coastal surface currents during CODE: the method and descriptive view. *J. Geophys. Res.* 90:4741–55
- Davis, RE, Dufour JE, Parks GJ, Perkins MR. 1982. Two inexpensive current-following drifters. Ref. 83-4, 74pp., Scripps Inst. Oceanogr., La Jolla, Calif.
- d’Ovidio F, Fernández V, Hernández-García E, López C. 2004. Mixing structures in the Mediterranean Sea from finite-size Lyapunov exponents. *Geophys. Res. Lett.* 31:L17203
- Ducet N, Le Traon PY, Reverdin G. 2000. Global high-resolution mapping of ocean circulation from TOPEX/Poseidon and ERS-1 and -2. *J. Geophys. Res.* 105:19477
- Eliot S, Gille ST. 2009. Estimates of wind energy input to the Ekman layer in the Southern Ocean from surface drifter data. *J. Geophys. Res. Oceans* 114:C06003

- Elipot S, Lumpkin R. 2008. Spectral description of oceanic near-surface variability. *Geophys. Res. Lett.* 35:L05605
- Elipot S, Lumpkin R, Perez R, Lilly J, Early J, Sykulski A. 2016. A global surface drifter dataset at hourly resolution. *J. Geophys. Res. Oceans.* 121.
- Emery WJ, Baldwin DJ, Schluskel P, Reynolds RW. 2001. Accuracy of in situ sea surface temperatures used to calibrate infrared satellite measurements. *J. Geophys. Res.* 106:2387–405
- Fox-Kemper B, Ferrari R, Hallberg RW. 2008. Parameterization of mixed layer eddies. Part I: theory and diagnosis. *J. Phys. Oceanogr.* 38:1145–65
- Garrett JF. 1980. The availability of the FGGE drifting buoy system data set. *Deep-Sea Res. A* 27:1083–86
- GHRSSST (Group High Resolut. Sea Surf. Temp.). 2011. *DBCP-GHRSSST - pilot project to upgrade elements of the global drifting buoy fleet to allow the reporting of higher resolution SST and position.* <http://www.ghrsst.org/ghrsst/tags-and-wgs/stval-wg/dbcp-ghrsst-pilot-project>
- Haller G, Poje A. 1998. Finite time transport in aperiodic flows. *Phys. D* 119:352–80
- Haller G, Yuan G. 2000. Lagrangian coherent structures and mixing in two-dimensional turbulence. *Phys. D* 147:352–70
- Haza AC, Griffa A, Martin P, Molcard A, Özgökmen TM, et al. 2007. Model-based directed drifter launches in the Adriatic Sea: results from the DART Experiment. *Geophys. Res. Lett.* 34:L10605

- Haza AC, Özgökmen TM, Griffa A, Garraffo Z, Piterbarg L. 2012. Parameterization of particle transport at submesoscales in the Gulf Stream region using Lagrangian subgrid-scale models. *Ocean Model.* 42:31–49
- Haza AC, Özgökmen TM, Griffa A, Poje AC, Lelong P. 2014. How does drifter position uncertainty affect ocean dispersion estimates? *J. Ocean. Atmos. Technol.* 31:2809–28
- Haza AC, Özgökmen TM, Hogan P. 2016. Impact of submesoscales on surface material distribution in a Gulf of Mexico mesoscale eddy. *Ocean Model.* In review.
- Haza AC, Poje A, Özgökmen TM, Martin P. 2008. Relative dispersion from a high-resolution coastal model of the Adriatic Sea. *Ocean Model.* 22:48–65
- Heavey S, Rucker P, Stephenson E. 2015. U.S. says BP to pay \$20 billion in fines for 2010 oil spill. *Reuters*, Oct. 5. <http://www.reuters.com/article/us-bp-usa-idUSKCN0RZ14A20151005>
- Herbers THC, Jessen PF, Janssen TT, Colbert DB, MacMahan JH. 2012. Observing ocean surface waves with GPS-tracked buoys. *J. Atmos. Ocean. Technol.* 29:944–59
- Hormann V, Centurioni LR, Rainville L, Lee CM, Braasch LJ. 2014a. Response of upper ocean currents to Typhoon Fanapi. *Geophys. Res. Lett.* 41:3995–4003
- Hormann V, Centurioni LR, Reverdin G. 2014b. Evaluation of drifter salinities in the subtropical North Atlantic. *J. Atmos. Ocean. Technol.* 32:185–92
- Hormann V, Lumpkin R, Foltz G. 2012. Interannual north equatorial countercurrent variability and its relation to tropical Atlantic climate modes. *J. Geophys. Res.* 117:C04035
- Huntley H, Lipphardt BL Jr., Jacobs GA, Kirwan AD Jr. 2015. Clusters, deformation, and dilation: diagnostics for material accumulation regions. *J. Geophys. Res. Oceans* 120:6622–36

- IOC (Intergov. Oceanogr. Comm.), WMO (World Meteorol. Organ.). 1988. *Guide to drifting data buoys*. Man. Guides 20, UNESCO (UN Educ. Sci. Cult. Organ.), Paris.
- Jacobs GA, Huntley HS, Kirwan JAD, Lipphardt BL Jr., Campbell T, et al. 2015. Ocean processes underlying surface clustering. *J. Geophys. Res. Oceans* 121:180–97
- Jernelöv A, Lindén O. 1981. IXTOC I: a case study of the world's largest oil spill. *Ambio* 10:299–306
- Johnson GC. 2001. The Pacific Ocean subtropical cell surface limb. *Geophys. Res. Lett.* 28:1771–74
- Kaplan D, Largier J, Botsford L. 2005. HF radar observations of surface circulation off Bodega Bay (northern California, USA). *J. Geophys. Res.* 110:C10020
- Kennedy JJ, Smith RO, Rayner NA. 2012. Using AATSR data to assess the quality of in situ sea-surface temperature observations for climate studies. *Remote Sens. Environ.* 116:79–92
- Kent EC, Challenor PG. 2006. Toward estimating climatic trends in SST. Part II: random errors. *J. Atmos. Ocean. Technol.* 23:476–86
- Klein P, Lapeyre G. 2009. The oceanic vertical pump induced by mesoscale and submesoscale turbulence. *Annu. Rev. Mar. Sci.* 1:351–75
- Kolmogorov A. 1941. Dissipation of energy in locally isotropic turbulence. *Proc. Math. Phys. Sci.* 434:15–17
- Koszalka I, LaCasce JH, Andersson M, Orvik KA, Mauritzen C. 2011. Surface circulation in the Nordic Seas from clustered drifters. *Deep-Sea Res. I* 58:468–85
- Koszalka I, LaCasce JH, Orvik KA. 2009. Relative dispersion statistics in the Nordic Seas. *J. Mar. Res.* 67:411–33

- Kukulka T, Plueddemann AJ, Trowbridge JH, Sullivan PP. 2010. Rapid mixed layer deepening by the combination of Langmuir and shear instabilities: a case study. *J. Phys. Oceanogr.* 40:2381–400
- LaCasce JH. 2008. Statistics from Lagrangian observations. *Prog. Oceanogr.* 77:1–29
- LaCasce JH, Bower A. 2000. Relative dispersion in the subsurface North Atlantic. *J. Mar. Res.* 58:863–94
- LaCasce JH, Ohlmann C. 2003. Relative dispersion at the surface of the Gulf of Mexico. *J. Mar. Res.* 61:285–312
- Lagerloef GSE, Mitchum GT, Lukas RB, Niiler PP. 1999. Tropical Pacific near-surface currents estimated from altimeter, wind, and drifter data. *J. Geophys. Res.* 104:23313–26
- Lebedev K, Yoshinari H, Maximenko NA, Hacker PW. 2007. *YoMaHa'07: velocity data assessed from trajectories of Argo floats at parking level and at the sea surface*. Tech. Note 4(2), Int. Pac. Res. Cent., Univ. Hawaii, Honolulu
- Ledwell JR, Montgomery ET, Polzin KL, St. Laurent LC, Schmitt RW, Toole JM. 2000. Evidence for enhanced mixing over rough topography in the abyssal ocean. *Nature* 403:179–182
- Ledwell JR, Watson AJ, Law C. 1998. Mixing of a tracer in the pycnocline. *J. Geophys. Res.* 103:21499–529
- Leibovich S, Tandon A. 1993. Three-dimensional Langmuir circulation instability in a stratified layer. *J. Geophys. Res. Oceans* 98:16501–7
- Lipa B, Whelan C, Rector B, Nyden B. 2009. HF radar bistatic measurement of surface current velocities: drifter comparisons and radar consistency checks. *Remote Sens.* 1:1190–211
- Lippsett L. 2014. Message bottled in an email: a long-lost legacy of ocean research resurfaces. *Oceanus*, Feb. 6. <http://www.whoi.edu/oceanus/feature/bumpus>

- Lumpkin R. 2003. Decomposition of surface drifter observations in the Atlantic Ocean. *Geophys. Res. Lett.* 30:1753
- Lumpkin R, Centurioni L, Perez RC. 2016. Fulfilling observing system implementation requirements with the global drifter array. *J. Atmos. Ocean. Technol.* 33:685–95
- Lumpkin R, Elipot S. 2010. Surface drifter pair spreading in the North Atlantic. *J. Geophys. Res. Oceans* 115:C12017
- Lumpkin R, Flament P. 2013. On the extent and energetics of the Hawaiian Lee Countercurrent. *Oceanography* 26(1):58–65
- Lumpkin R, Garzoli SL. 2011. Interannual to decadal variability in the southwestern Atlantic’s surface circulation. *J. Geophys. Res. Oceans* 116:C01014
- Lumpkin R, Grodsky S, Rio M-H, Centurioni L, Carton J, Lee D. 2013. Removing spurious low-frequency variability in surface drifter velocities. *J. Atmos. Ocean. Technol.* 30:353–60
- Lumpkin R, Johnson G. 2013. Global ocean surface velocities from drifters: mean, variance, ENSO response, and seasonal cycle. *J. Geophys. Res. Oceans* 118:2992- 3006
- Lumpkin R, Maximenko N, Pazos M. 2012. Evaluating where and why drifters die. *J. Atmos. Ocean. Technol.* 29:300–8
- Lumpkin R, Pazos M. 2007. Measuring surface currents with Surface Velocity Program drifters: the instrument, its data, and some recent results. In *Lagrangian Analysis and Prediction of Coastal and Ocean Dynamics*, ed. A Griffa, AD Kirwan, A Mariano, T Özgökmen, T Rossby, pp. 39–67. Cambridge, UK: Cambridge Univ. Press
- Mancho A, Hernández-García E, Small D, Wiggins S, Fernández V. 2008. Lagrangian transport through an ocean front in the northwestern Mediterranean Sea. *J. Phys. Oceanogr.* 38:1222–37

- Maximenko N, Hafner J, Niiler P. 2012. Pathways of marine debris derived from trajectories of Lagrangian drifters. *Mar. Pollut. Bull.* 65:51–62
- Maximenko N, Lumpkin R, Centurioni L. 2014. Ocean surface circulation. In *Ocean Circulation and Climate: A 21st Century Perspective*, ed. G Siedler, SM Griffies, J Gould, JA Church, pp. 283–300. Oxford, UK: Academic Press. 2nd ed.
- McCarty JF. 2015. Toxic algae threatens Lake Erie drinking water, but Toledo has the new technology to cope. *Cleveland Plain Dealer*, July 30.
http://www.cleveland.com/metro/index.ssf/2015/07/toxic_algae_threatens_lake_eri.html
- McNally GJ, Luther DS, White WB. 1989. Subinertial frequency response of wind-driven currents in the mixed layer measured by drifting buoys in the midlatitude North Pacific. *J. Phys. Oceanogr.* 19:290–300
- McNally GJ, Patzert WC, Kirwan JAD, Vastano AC. 1983. The near-surface circulation of the North Pacific using satellite tracked drifting buoys. *J. Geophys. Res.* 88:7634–40
- McWilliams JC. 2008. Fluid dynamics at the margin of rotational control. *Environ. Fluid Mech.* 8:441–49
- Mensa J, Griffa A, Garraffo Z, Özgökmen T, Haza A, Veneziani M. 2013. Seasonality of the submesoscale dynamics in the Gulf Stream region. *Ocean Dyn.* 63:923–41
- Mezić I, Wiggins S. 1994. On the integrability and perturbation of three-dimensional fluid flows with symmetry. *J. Nonlinear Sci.* 4:157–94
- Monin A, Yaglom A. 1965 (2007). *Statistical Fluid Mechanics: Mechanics of Turbulence*, Vol. I. Mineola, NY: Dover.
- Niiler PP. 2001. The world ocean surface circulation. In *Ocean Circulation and Climate: Observing and Modelling the Global Ocean*, ed. G Siedler, J Church, J Gould, pp. 193–204. Oxford, UK: Academic Press

- Niiler PP. 2003. *A brief history of drifter technology*. Presented at the Autonomous and Lagrangian Platforms and Sensors Workshop, Scripps Inst. Oceanogr., La Jolla, CA, March 31-April 2, 2003.
- Niiler PP, Davis R, White H. 1987. Water-following characteristics of a mixed-layer drifter. *Deep-Sea Res. A* 34:1867–82
- Niiler PP, Maximenko N, Panteleev GG, Yamagata T, Olson DB. 2003. Near-surface dynamical structure of the Kuroshio Extension. *J. Geophys. Res.* 108:3193
- Niiler PP, Paduan JD. 1995. Wind-driven motions in the northeastern Pacific as measured by Lagrangian drifters. *J. Phys. Oceanogr.* 25:2819–30
- Normile D. 2014. Lost at sea. *Science* 344:963–965
- Novelli G, Guigand CC, Özgökmen TM, Cousin C, Haus B. 2016. A biodegradable surface drifter for ocean sampling on a massive scale: design, calibration, and application. *J. Atmos. Ocean. Technol.* In review.
- Ohlmann C, White P, Washburn L, Terrill E, Emery B, Otero M. 2007. Interpretation of coastal HF radar-derived surface currents with high-resolution drifter data. *J. Atmos. Ocean. Technol.* 24:666–80
- Okubo A. 1970. Horizontal dispersion of floatable particles in the vicinity of velocity singularities such as convergences. *Deep-Sea Res. Oceanogr. Abstr.* 17:445–54
- Olascoaga MJ, Beron-Vera FJ, Haller G, Trénes J, Iskandarani M, et al. 2013. Drifter motion in the Gulf of Mexico constrained by altimetric Lagrangian coherent structures. *Geophys. Res. Lett.* 40:6171–75
- Olascoaga MJ, Haller G. 2012. Forecasting sudden changes in environmental pollution patterns. *PNAS* 109:4738–43

- Olascoaga MJ, Rypina II, Brown MG, Beron-Vera FJ, Koçak H, et al. 2006. Persistent transport barrier on the West Florida Shelf. *Geophys. Res. Lett.* 33:L22603
- Ollitrault M, Gabillet C, de Verdière AC. 2005. Open ocean regimes of relative dispersion. *J. Fluid Mech.* 533:381–407
- Ottino J. 1989. *The Kinematics of Mixing: Stretching, Chaos and Transport*. Cambridge, UK: Cambridge Univ. Press
- Özgökmen TM, Fischer PF. 2012. CFD application to oceanic mixed layer sampling with Lagrangian platforms. *Int. J. Comput. Fluid Dyn.* 26:337–48
- Özgökmen TM, Poje A, Fischer P. 2012. On multi-scale dispersion under the influence of surface mixed layer instabilities and deep flows. *Ocean Model.* 56:16–30
- Özgökmen TM, Poje A, Fischer P, Haza A. 2011. Large eddy simulations of mixed layer instabilities and sampling strategies. *Ocean Model.* 39:311–31
- Paduan J, Rosenfeld L. 1996. Remotely sensed surface currents in Monterey Bay from shore based HF radar (Coastal Ocean Dynamics Application Radar). *J. Geophys. Res.* 101:20669–86
- Park JJ, Kim K, Crawford WR. 2004. Inertial currents estimated from surface trajectories of Argo floats. *Geophys. Res. Lett.* 31:L13307
- Park JJ, Kim K, King B. 2005. Global statistics of inertial motion. *Geophys. Res. Lett.* 32:L14612
- Pazan SE, Niiler PP. 2001. Recovery of near-surface velocity from undrogued drifters. *J. Atmos. Ocean. Technol.* 18:476–89
- Pinsky C. 2013. Sending out an S.O.S. *New York*, July 14.
<http://nymag.com/news/intelligencer/topic/solo-message-in-a-bottle-2013-7>

- Poje A, Haller G. 1999. Geometry of cross-stream mixing in a double-gyre ocean model. *J. Phys. Oceanogr.* 29:1649–65
- Poje A, Haza A, Özgökmen T, Magaldi M, Garraffo Z. 2010. Resolution dependent relative dispersion statistics in a hierarchy of ocean models. *Ocean Model.* 31:36–50
- Poje AC, Özgökmen TM, Lipphardt BL Jr., Haus BK, Ryan EH, et al. 2014. Submesoscale dispersion in the vicinity of the *Deepwater Horizon* oil spill. *PNAS* 111:12693–98
- Pratt L, Rypina I, Özgökmen TM, Wang P, Childs H, Bebieva Y. 2013. Chaotic advection in a steady, three-dimensional, Ekman-driven eddy. *J. Fluid Mech.* 738:087401
- Provenzale A. 1999. Transport by coherent barotropic vortices. *Annu. Rev. Fluid Mech.* 31:55–93
- Ralph EA, Niiler PP. 1999. Wind-driven currents in the tropical Pacific. *J. Phys. Oceanogr.* 29:2121–29
- Richardson LF. 1926. Atmospheric diffusion shown on a distance-neighbour graph. *Proc. R. Soc. Lond. A* 110:709–37
- Richardson LF, Stommel H. 1948. Note on eddy diffusion in the sea. *J. Meteorol.* 5:238–40
- Rio MH, Hernandez F. 2003. High-frequency response of wind-driven currents measured by drifting buoys and altimetry over the world ocean. *J. Geophys. Res. Oceans* 108:3283
- Rypina II, Jayne S, Yoshida S, Macdonald A, Buesseler K. 2014a. Drifter-based estimate of the 5 year dispersal of Fukushima-derived radionuclides. *J. Geophys. Res.* 119:8177–93
- Rypina II, Kirincich AR, Limeburner R, Udovydchenkov IA. 2014b. Eulerian and Lagrangian correspondence of high-frequency radar and surface drifter data: effects of radar resolution and flow components. *J. Atmos. Ocean. Technol.* 31:945–66
- Rypina II, Pratt L, Wang P, Özgökmen TM, Mezic I. 2015. Resonance phenomena in 3D time-dependent volume-preserving flows with symmetries. *Chaos* 25:143–83

Sanford T, Kelly K, Farmer D. 2011. Sensing the ocean. *Phys. Today* 64:24–28

Sasaki H, Klein P, Qiu B, Sasai Y. 2014. Impact of oceanic-scale interactions on the seasonal modulation of ocean dynamics by the atmosphere. *Nat. Commun.* 5:5636

Schmidt WE, Woodward BT, Millikan KS, Guza RT, Raubenheimer B, Elgar S. 2003. A GPS-tracked surf zone drifter. *J. Atmos. Ocean. Technol.* 20:1069–75

Schroeder K, Chiggiato J, Haza AC, Griffa A, Özgökmen TM, et al. 2012. Targeted Lagrangian sampling of submesoscale dispersion at a coastal frontal zone. *Geophys. Res. Lett.* 39:L11608

Schroeder K, Haza AC, Griffa A, Özgökmen TM, Poulain P, et al. 2011. Relative dispersion in the Liguro-Provençal basin: from sub-mesoscale to mesoscale. *Deep-Sea Res. I* 58:861–82

Shay L, Cook T, An P. 2003. Submesoscale coastal ocean flows detected by very high frequency radar and autonomous underwater vehicles. *J. Atmos. Ocean. Technol.* 20:1583–600

Shay L, Martinez-Pedraja J, Cook T, Haus B. 2007. High-frequency radar mapping of surface currents using WERA. *J. Atmos. Ocean. Technol.* 24:484–503

Shcherbina AY, D’Asaro EA, Lee CM, Klymak JM, Molemaker MJ, McWilliams JC. 2013. Statistics of vertical vorticity, divergence, and strain in a developed submesoscale turbulence field. *Geophys. Res. Lett.* 40:4706–11

Skyllingstad E, Denbo D. 1995. An ocean large-eddy simulation of Langmuir circulations and convection in the surface mixed layer. *J. Geophys. Res. Oceans* 100:8501–22

Sotillo MG, Garcia-Ladona E, Orfila A, Rodríguez-Rubio P, Maraver JC, et al. 2016. The MEDESS-GIB database: tracking the Atlantic water inflow. *Earth Syst. Sci. Data* 8:141–49

- Staletovich J. 2016. FPL nuclear plant canals leaking into Biscayne Bay, study confirms. *Miami Herald*, Mar. 7.
- <http://www.miamiherald.com/news/local/environment/article64667452.html>
- Steward R, Joy J. 1974. HF radio measurements of surface currents. *Deep-Sea Res. Oceanogr. Abstr.* 21:1039–49
- Stommel H. 1949. Horizontal diffusion due to oceanic turbulence. *J. Mar. Res.* 8:199-225
- Sturges W, Niiler PP, Weisberg RH. 2001. *Northeastern Gulf of Mexico inner shelf circulation study*. OCS Rep. MMS 2001-103, Miner. Manag. Serv., US Dep. Interior, Herndon, VA
- Sundermeyer MA, Skillingstad E, Ledwell JR, Concannon B, Terray EA. 2014. Observations and numerical simulations of large-eddy circulation in the ocean surface mixed layer. *Geophys. Res. Lett.* 41:7584–90
- Sundermeyer MA, Terray EA, Ledwell JR, Cunningham AG, LaRocque PE, et al. 2007. Three-dimensional mapping of fluorescent dye using a scanning, depth-resolving airborne radar. *J. Atmos. Ocean. Technol.* 24:1050–65
- Sybrandy AL, Niiler PP. 1992. *WOCE/TOGA Lagrangian drifter construction manual*. WOCE Rep. 63, SIO Ref. 91/6, Scripps Inst. Oceanogr., La Jolla, CA
- Taylor G. 1921. Diffusion by continuous movements. *Proc. Lond. Math. Soc.* 20:196– 212
- Taylor JR, Ferrari R. 2010. Buoyancy and wind-driven convection at mixed layer density fronts. *J. Phys. Oceanogr.* 40:1222–42
- Thomas L, Tandon A, Mahadevan A. 2008. Submesoscale processes and dynamics. In *Ocean Modeling in an Eddy Regime*, ed. MW Hecht, H Hasume, pp. 17–38. Washington, DC: Am. Geophys. Union

- US Coast Guard. 2013. *U.S. Coast Guard Addendum to the United States National Search and Rescue Supplement (NSS) to the International Aeronautical and Maritime Search and Rescue Manual (IAMSAR)*. Command. Instr. M16130.2F, US Coast Guard, US Dep. Homel. Secur., Washington, DC
- Van Roekel LP, Fox-Kemper B, Sullivan PP, Hamlington PE, Haney SR. 2012. The form and orientation of Langmuir cells for misaligned winds and waves. *J. Geophys. Res. Oceans* 117:C05001
- Van Sebille E, Wilcox C, Lebreton L, Maximenko N, Hardesty BD et al. 2015. A global inventory of small floating plastic debris. *Environmental Res. Lett.* 10:124006.
- WCRP (World Clim. Res. Programme). 1988. *World Ocean Circulation Experiment Surface Velocity Programme Planning Committee report of the first meeting: SVP-1 and TOGA pan-Pacific surface current study*. WCRP-26 (WMO/TD-No. 323), World Meteorol. Organ., Wormley, UK
- Wunsch C, Stammer D. 1998. Satellite altimetry, the marine geoid, and the oceanic general circulation. *Annu. Rev. Earth Planet. Sci.* 26:219–53
- Zhang H-M, Reynolds RW, Lumpkin R, Molinari R, Arzayus K, et al. 2009. An Integrated Global Ocean Observing System for sea surface temperature using satellites and in situ data: research to operations. *Bull. Am. Meteorol. Soc.* 90:31–38
- Zhong Y, Bracco A, Villareal T. 2012. Pattern formation at the ocean surface: *Sargassum* distribution and the role of the eddy field. *Limnol. Oceanogr. Fluid Environ.* 2:12–27



Figure 1. A Surface Velocity Program (SVP) drifter, with author Rick Lumpkin for scale reference. At left is the holey-sock drogue, centered at a depth of 15 m when the instrument is deployed. The drogue is attached to the surface float (*bottom right*) by a tether, much of which is bound by paper tape inside a cardboard tube for ease of deployment.

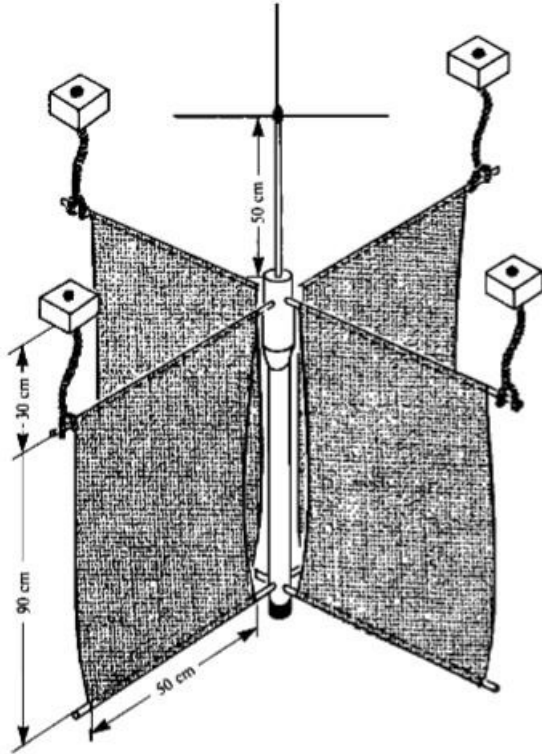


Figure 2. Diagram of the Coastal Ocean Dynamics Experiment surface drifter (a.k.a. Davis drifter). Reproduced from Davis (1985) with permission from the author.



Figure 3. (a) A biodegradable Lagrangian Submesoscale Experiment (LASER) drifter. (b) LASER drifter testing in the University of Miami wave tank. (c) A LASER drifter being used during an oil spill exercise. Images provided by the Consortium for Advanced Research on Transport of Hydrocarbon in the Environment (<http://carthe.org>).

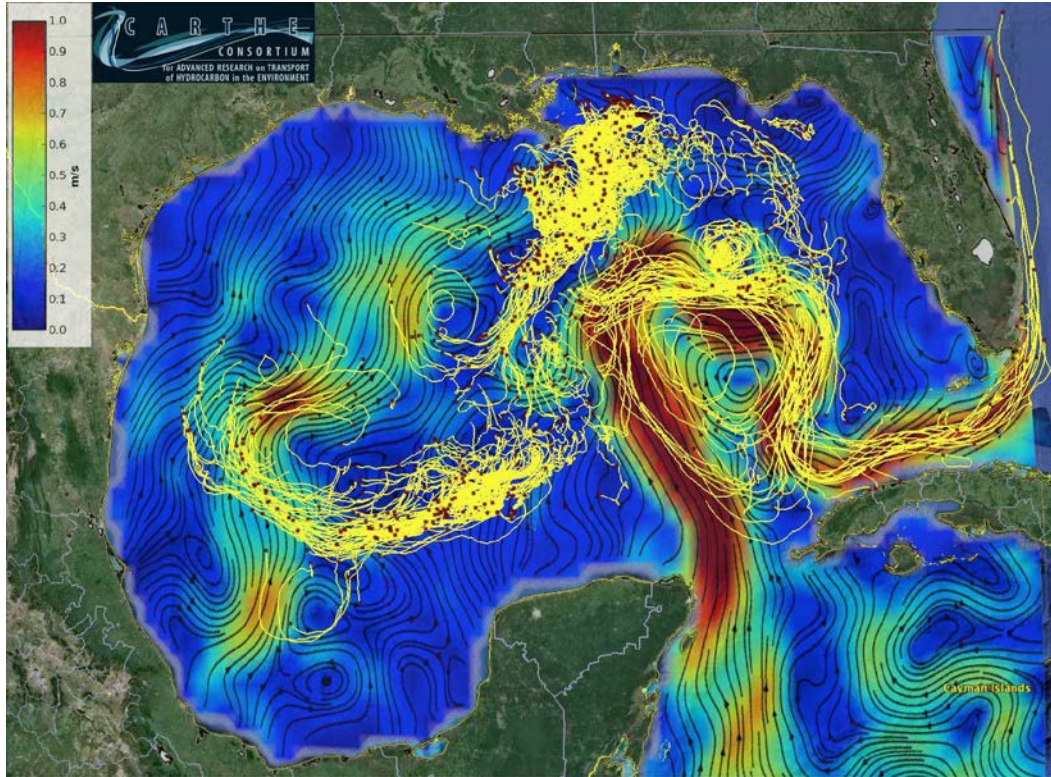


Figure 4. Trajectories of biodegradable Lagrangian Submesoscale Experiment (LASER) drifters in the Gulf of Mexico superimposed on surface currents. The red squares mark drifter positions on March 9, 2016; the tails are 14 days long. The surface speed field was derived from sea surface height anomaly and Ekman drift corresponding to March 9, 2016. Adapted from AVISO (2016).

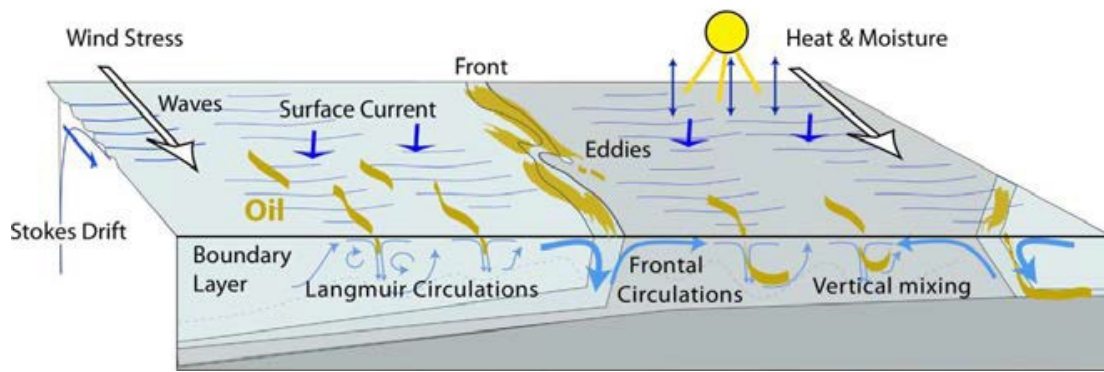


Figure 5. (a). Surface oil during the *Deepwater Horizon* spill. Photo courtesy of Daniel Beltra. (b) Schematic of upper-ocean transport processes.